arXiv:1903.10648v1 [cond-mat.mes-hall] 26 Mar 2019

Plasmon Resonances and Tachyon Ghost Modes in Highly Conducting Sheets

D. O. Oriekhov[1] and L. S. Levitov[2]

[1]*Department of Physics, Taras Shevchenko National University of Kiev, Kiev, 03680, Ukraine*
[2]*Massachusetts Institute of Technology, Cambridge, Massachusetts 02139, USA*

Plasmon-polariton modes in two-dimensional electron gases are bound states of field and matter with unusual properties. For electrical conductivity exceeding a certain threshold value these modes display an interesting relation with tachyons, the hypothetical faster-than-light particles. While not directly observable, tachyons affect properties of other excitations. In the "tachyon" regime, plasmon resonances remain sharp even when the carrier collision rate γ exceeds plasmon resonance frequency. Resonances feature a recurrent behavior as γ increases, first broadening and then narrowing and acquiring asymmetric non-Lorentzian lineshapes with power-law tails extending into the tachyon continuum $\omega > ck$. Narrow resonances persisting for $\gamma > \omega$, along with the unusual density and temperature dependence of resonance frequencies, provide clear signatures of the tachyon regime.

Surface plasmons in atomically thin electron systems feature a number of interesting and potentially useful properties, such as strong light-matter interaction and field confinement, as well as gate tunability[1–6]. Plasmon modes, owing to their hybrid charge-field character, enable powerful diagnostic for electronic properties of two-dimensional (2D) materials[7, 8]. The synchronized movement of charge in different spatial regions, which constitutes plasmons, is sustained by long-range electron-electron interactions. In that, the effects of EM retardation due to the finite speed of light are typically small, since electron velocities in solids are nonrelativistic[9]. Yet, since models based on nonretarded Coulomb interaction predict $\omega \sim \sqrt{k}$ dispersion with group velocity diverging at small k, the relativistic retardation effects are guaranteed to become prominent in the long-wavelength limit. Strong retardation gives rise to plasmon-polariton modes which represent 3D/2D field-matter bound states with novel properties[10–12].

Can retardation-dominated modes be accessed without changing plasmon wavelength? This question was first posed by Falko and Khmelnitskii[13], who predicted enhancement of retardation effects upon increasing the conductivity of the electron gas. Ref.[13] also uncovered a truly puzzling behavior — collective modes resembling tachyons, the hypothetical superluminal particles. The regime of interest is reached when the DC ohmic conductivity exceeds the threshold set by the speed of light:

$$\sigma_0 > c/2\pi. \tag{1}$$

In cgs units, used in Eq.(1), ohmic conductivity has dimension of velocity, wherein $2\pi/c \approx 188\,\Omega$ per square[14]. Such values are routinely reachable in state-of-the-art 2D electron systems[10–12]; in SI units Eq.(1) reads $\sigma_0 > 2\varepsilon_0 c$. Ref.[13], by analyzing the dynamics of 2D currents coupled to 3D EM field, obtained modes which, if taken for granted, would describe excitations traveling at superluminal speeds. This would of course violate the known laws of physics, leading to a conclusion that these are some kind of ghost modes that cannot be observed directly. Despite several attempts to clarify the meaning of these findings[11, 12, 15], their relation to observable quantities has remained uncertain.

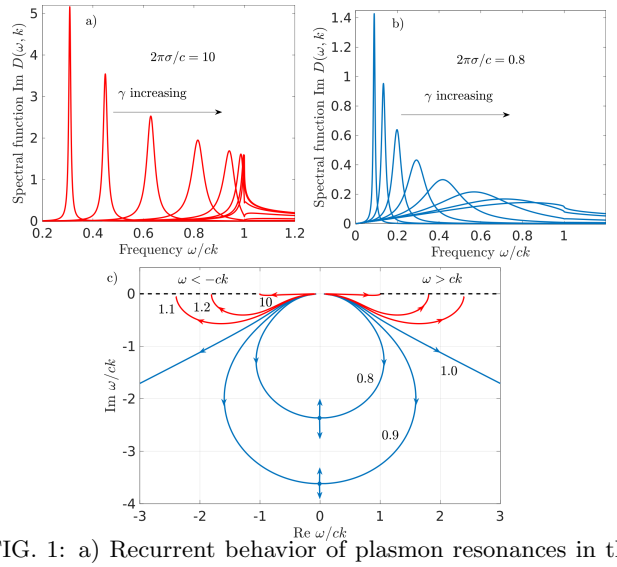

FIG. 1: a) Recurrent behavior of plasmon resonances in the "tachyon" regime $\sigma_0 > c/2\pi$. Plotted is the dynamic compressibility $\mathrm{Im}\, D(\omega,k)$, Eq.(2), at a fixed σ_0. Resonances evolve nonmonotonically as the collision rate γ grows, first broadening, then sharpening and developing non-Lorentzian lineshapes, while the resonance frequency becomes pinned at $\omega \approx ck$ value. b) Non-recurrent behavior at $\sigma_0 < c/2\pi$: resonances broaden and become overdamped as γ increases. c) Pole trajectories, obtained from Eq.(4) at a fixed σ_0. Arrows show the direction of pole movement at increasing γ; numbers indicate $2\pi\sigma_0/c$ values. For $2\pi\sigma_0 > c$, the poles move under the branch cuts of the square roots in Eq.(2) (dashed lines). Positioned under branch cuts, the poles represent the Falko-Khmelnitskii tachyons, Eq.(7). The latter, despite being undamped, $\mathrm{Im}\,\omega = 0$, do not produce propagating modes.

With this motivation in mind, here we analyze plasmon resonances and their relation to tachyon modes. We focus on the charge-potential linear response function of a 2D conducting sheet, $\rho_{\omega,k} = -D(\omega,k)\phi_{\omega,k}$. The dynamical compressibility $D(\omega,k)$ is found to be expressed through the dispersive sheet conductivity $\sigma(\omega)$ as

$$D(\omega,k) = \frac{k^2\sigma(\omega)}{2\pi q(\omega)\sigma(\omega) - i\omega}, \quad q(\omega) = \sqrt{k^2 - \frac{\omega^2}{c^2}}. \tag{2}$$

The dielectric constant of the surrounding medium, ignored here for simplicity, will be accounted for below, see Eq.(18).

The spectral function $\mathrm{Im}\, D(\omega, k)$ describes plasmon resonances in several different regimes. At $\sigma_0 > c/2\pi$, the resonances acquire an interesting recurrent character, which is illustrated in Fig.1. As the collision rate γ grows, with the conductivity σ_0 and wavenumber k values kept fixed, resonances first broaden, but then, when γ exceeds ck, they sharpen as γ increases. Simultaneously, resonance frequency becomes pinned at $\omega = ck$ value and lineshapes change from Lorentzian to highly non-Lorentzian. Strikingly, resonances remain sharp even when the collision rate γ is much greater than the resonance frequency ω. In this regime, lineshapes become asymmetrical, cuspy, and develop tails extending far in the $\omega > ck$ continuum. At $\sigma_0 < c/2\pi$, in contrast, a conventional behavior takes place: resonances broaden when γ grows and are quickly washed out.

The physical reason for resonances sharpening can be understood as a reduction in damping due to a change in the mode makeup upon frequency approaching ck. Indeed, at $\omega < ck$ the field outside the conducting sheet represents an evanescent wave decaying as a function of distance as $e^{-\lambda z}$ with the decay parameter $\lambda = q(\omega)$. Since the latter becomes small as ω approaches ck, the mode confinement in the direction perpendicular to the plane becomes less tight, leading to an enhancement in the field-matter volume ratio. This makes the mode overlap with two-dimensional electrons smaller and, therefore, reduces damping. Here and below we assume that dissipation is dominated by ohmic losses of 2D electrons; the situation in experimental systems can be more complicated due to losses in the surrounding medium.

In experiment, the key system parameters – γ and σ_0 – can be varied independently by tuning temperature and carrier density (T and n). However, since in general the T and n dependence of γ and σ_0 may be fairly complicated, here it will be convenient to view these quantities as proxies for the experimental knobs, treating them as independently tunable variables. This represents a meaningful choice also because the quantity σ_0 is directly measurable, and thus the recurrent evolution of resonances at a fixed σ_0 and varying γ, such as that shown in Figs.1 and 2, can be extracted directly from the measurement results without knowing the exact dependence of γ and σ_0 on the experimental knobs such as T and n.

More insight into the properties of the resonances, in particular their relation with the tachyon modes of Ref.[13], can be gained by investigating poles of $D(\omega, k)$, which we analyze for the dispersive Drude model:

$$i\omega = 2\pi q(\omega)\sigma(\omega), \quad \sigma(\omega) = \frac{ne^2}{m(\gamma - i\omega)}, \tag{3}$$

The dispersion relation (3), after simple algebra, yields a characteristic equation

$$\frac{\omega^2(\omega + i\gamma)^2}{\beta^2} + \frac{\omega^2}{c^2} = k^2, \quad \beta = \frac{2\pi ne^2}{m}. \tag{4}$$

This quartic equation has four complex roots that can be found explicitly from the general quartic formula (the Ferrari-Cardano method). Only two of these roots, however, are the poles of $D(\omega, k)$ that are shown in Fig.1(c). Two spurious roots, added when the square root in $q(\omega)$ is rationalized, are discarded.

The behavior of poles in the complex ω plane, which is illustrated in Fig.1(c), mimics the recurrent behavior of resonances in the "tachyon" regime $\sigma_0 > c/2\pi$: as γ increases and σ_0 is kept fixed, the poles first move away from the real ω axis, then make a U-turn and move back towards the real axis, landing on the lower side of the branch cuts $\omega < -ck$ and $\omega > ck$. Likewise, at $\sigma_0 < c/2\pi$ pole trajectories show a non-recurrent behavior: moving gradually away from the real axis without turning back, and then colliding at the imaginary axis to create a pair of overdamped modes with pure imaginary ω.

Quantitatively, this behavior can be described most easily by taking the limit $2\pi\sigma_0 \gg c$ in Eq.(4). In this case, as Fig.1 suggests, the real part of ω is much greater than the imaginary part. Ignoring the latter at first, we take the $\omega \gg \gamma$ limit. This yields a dependence

$$k^2 = \frac{\omega^4}{\beta^2} + \frac{\omega^2}{c^2}, \tag{5}$$

which gives the dispersion $\omega = (\beta k)^{1/2}$ at large k, and a light-like dispersion $\omega = ck$ at small k, as expected. The imaginary part of ω, which provides an estimate for resonance width, can be found by replacing $\omega \to \omega - i\Gamma$, and expanding in small γ and Γ to first order. This gives

$$\Gamma = \frac{2\omega^2\gamma}{2\omega^2 + \frac{\beta^2}{c^2}}. \tag{6}$$

Substituting $\beta = 2\pi\sigma_0\gamma$ and taking σ_0 to be constant, we see that Eq.(6) predicts a nonmonotonic dependence for Γ vs. γ. For the resonance width, estimated as Γ, this behavior is in good agreement with the recurrent evolution of resonances and poles at varying γ and constant σ_0, as shown in Fig.1 and, in greater detail, in Fig.2.

At $2\pi\sigma_0 \gtrsim c$ and high damping γ, the poles of $D(\omega, k)$ are positioned directly beneath the branch cuts. In the limit $\gamma \gg \omega$, after approximating $\sigma(\omega) \approx \sigma_0 + \frac{i\omega}{\gamma}\sigma_0$, simple algebra gives

$$\omega_\pm = \pm vk - i\gamma', \quad v = \frac{c\alpha}{\sqrt{\alpha^2 - 1}}, \quad \alpha = \frac{2\pi\sigma_0}{c}, \tag{7}$$

the values identical to those found in Ref.[13], with damping $\gamma' = \frac{\alpha^2 c^2 k^2}{\gamma(\alpha^2-1)^2}$ vanishing at high γ. As noted in Ref.[13], the peculiar dispersion relation with greater-than-c group velocity does not imply superluminal signal

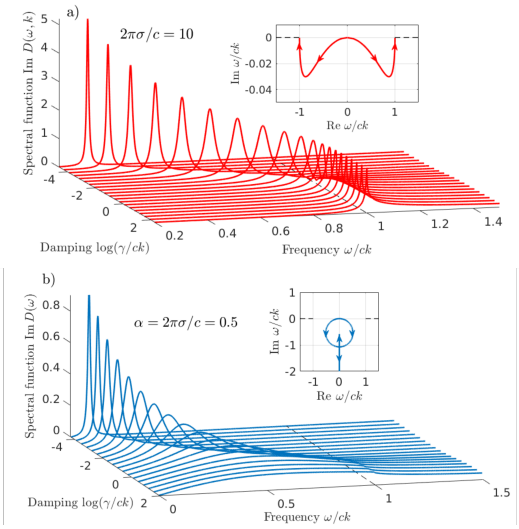

FIG. 2: Frame-by-frame evolution of the resonances in Fig.1. a) At a constant $\sigma_0 > c/2\pi$, resonances are dispersing as the collision rate grows from $\gamma \ll ck$ to $\gamma \sim ck$, and non-dispersing at $\gamma > ck$ after resonance frequency becomes pinned at the edge of the continuum $\omega > ck$, taking value $\omega \approx ck$. Resonance width vs. γ dependence is nonmonotonic, broadening while $\gamma < ck$ and narrowing once γ exceeds ck. b) Conventional behavior at $\sigma_0 < c/2\pi$: resonances broaden as γ grows and are washed out once γ exceeds the resonance frequency. Insets in a) and b) show the trajectories of $D(\omega,k)$ poles in the complex ω plane, obtained by varying γ.

propagation. The reasons for that, which are somewhat subtle, can be summarized as follows.

First, since at large γ the frequencies $\omega_\pm$ reside directly at the branch cuts $\omega > ck$ and $\omega < -ck$, the poles $\omega = \omega_\pm$ do not represent isolated singularities; rather the poles and branch cuts must be handled jointly as *compound*, or *unseparable,* singularities. Another point of note, which is more essential than the "compound singularity" property, is that the poles reside on the lower (unphysical) sides of the branch cuts, which separate the poles from the upper imaginary halfplane $\mathrm{Im}\,\omega > 0$. Since it is the ω dependence in that halfplane that governs time evolution of a response, the poles separated from the $\mathrm{Im}\,\omega > 0$ domain by branch cuts cannot create, on their own, any $v > c$ modes. More formally, below we demonstrate that these poles give no singular contributions to the spectral function because their residues vanish, see Eq.(11) and accompanying discussion. Instead, the poles under the branch cuts alter the shapes of the resonances positioned at $\omega \lesssim ck$, which remain sharp even when $\gamma \gg \omega$ but acquire asymmetric line shapes with the tails extending into the tachyon continuum $\omega > ck$.

To validate this picture, we consider the charge-potential response in the time domain:

$$\rho_k(t) = -\int_{-\infty}^{\infty} dt' D_k(t-t')\phi_k(t'), \tag{8}$$

corresponding to $\rho_{\omega,k} = -D(\omega,k)\phi_{\omega,k}$ at a fixed wavenumber k. The memory function $D_k(t-t')$ equals

$$D_k(\tau) = \int_{-\infty}^{\infty} \frac{d\omega}{2\pi} e^{-i\omega\tau} D(\omega,k). \tag{9}$$

Here the integral runs over a straight path $-\infty < \omega < \infty$ just above the real axis. The causality condition $D_k(\tau < 0) = 0$ is ensured, as always, by analyticity of $D(\omega,k)$ in the upper halfplane $\mathrm{Im}\,\omega > 0$.

To see why the expression in Eq.(2), when plugged in Eq.(9), does not generate propagating modes with $v > c$, we start with a simple technical observation regarding analytic properties of $q(\omega)$. The quantity $q(\omega)$ is real in the domain $-ck < \omega < ck$ and pure imaginary at $\omega > ck$ and $\omega < -ck$ with a sign that must be determined by analytic continuation. The recipe for continuation follows from analyticity of $q(\omega)$ in the halfplane $\mathrm{Im}\,\omega > 0$, prescribed by causality. Therefore, $q(\omega)$ should be treated as $\sqrt{k^2 - \frac{(\omega+i0)^2}{c^2}}$ with an infinitesimal positive shift in ω, giving

$$q(\omega) = \begin{cases} \sqrt{k^2 - \frac{\omega^2}{c^2}}, & -ck < \omega < ck \\ -i\,\mathrm{sgn}\,\omega \sqrt{\frac{\omega^2}{c^2} - k^2}, & \omega < -ck,\ \omega > ck \end{cases} \tag{10}$$

where the sign factor $-\mathrm{sgn}\,\omega$ for the cases $\omega > ck$ and $\omega < -ck$ arises due to analytic continuation through the upper halfplane. A simple consequence of this result is that the dispersion equation obtained in Ref.[13] does not have solutions at the real axis on the upper side of branch cuts. The solutions given in (7) are located under the cuts $\omega > ck$ and $\omega < -ck$. Therefore, from the point of view of analytical properties, they represent fictitious poles, or more precisely, the poles located on a non-physical sheet of the Riemann surface of complex frequency ω. As such, they do not generate propagating modes.

This point can be illustrated by transforming the expression in Eq.(2) in the $\gamma \gg \omega$ limit to the form

$$D(\omega,k) = \frac{\alpha c k^2 (\alpha\sqrt{c^2k^2 - \omega^2} + i\omega)}{\alpha^2 c^2 k^2 - (\alpha^2 - 1)\omega^2}, \tag{11}$$

where we replaced $\sigma(\omega)$ in Eq.(2) by $\sigma_0 = c\alpha/2\pi$, and rationalized denominator by multiplying it by $\alpha\sqrt{c^2k^2 - \omega^2} + i\omega$. This expression has poles on the real axis at the tachyon frequencies $\omega = \pm vk$ with $v > c$, Eq.(7), so long as $\alpha > 1$. However these poles give a vanishing contribution to the spectral function evaluated at $\mathrm{Im}\,\omega = +i0$ because the numerator, owing to the sign prescription found above, Eq.(10), vanishes at the poles. As a result, the spectral function is smooth at the tachyon frequencies $|\omega| > ck$. This is clearly seen in the resonances shown in Figs.1 and 2 which have smooth tails extending into the tachyon continuum with cusps at $\omega = ck$ but no singularities at $\omega > ck$.

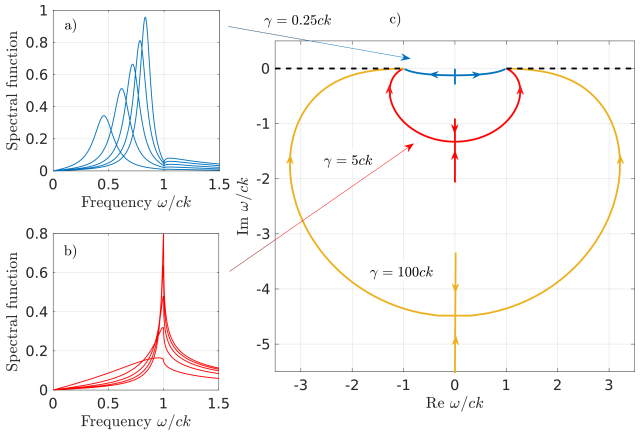

FIG. 3: a),b) Evolution of resonances at a fixed γ and $2\pi\sigma_0/c$ increasing from 1 to 5. Resonances sharpen as σ_0 increases; in b) they become very narrow despite that the resonance frequency remains smaller than γ. c) Pole trajectories found from Eq.(4) plotted at a fixed γ for $2\pi\sigma_0/c$ varying from 0.01 to 20. The direction of pole movement is indicated by arrows. The branch cuts $|\omega| > c|k|$ are shown by dashed lines; γ values are indicated next to arrows. Tachyon resonances arise at large σ_0 as the poles approach the branch cuts.

Next, we proceed to derive the response function given in Eq.(2) and estimate the relevant experimental parameter values. We start with EM equations in 3D space due to 2D currents, for generality adding a dielectric constant of the surrounding medium. Using Fourier harmonics, in Lorentz gauge we have $\boldsymbol{k}\cdot\boldsymbol{A}_{\boldsymbol{k},\omega} - \frac{\omega}{c}\varepsilon\phi_{\boldsymbol{k},\omega} = 0$, and

$$(\boldsymbol{k}^2 - \tfrac{\omega^2}{c^2}\varepsilon)\boldsymbol{A}_{\boldsymbol{k},\omega} = \frac{4\pi}{c}\boldsymbol{j}_{\boldsymbol{k},\omega}, \quad (\boldsymbol{k}^2 - \tfrac{\omega^2}{c^2}\varepsilon)\phi_{\boldsymbol{k},\omega} = \frac{4\pi}{\varepsilon}\rho_{\boldsymbol{k},\omega}.$$

Taking z axis to be perpendicular to the 2D sheet, and working in a mixed Fourier representation,

$$\phi_{\boldsymbol{k},\omega}(z) = \sum_{k_z}\phi_{\boldsymbol{k},\omega}e^{ik_z z}, \quad \rho_{\boldsymbol{k},\omega}(z) = \sum_{k_z}\rho_{\boldsymbol{k},\omega}e^{ik_z z},$$

where from now on $\boldsymbol{k}$ is two-dimensional, we have

$$(\partial_z^2 - k^2 + \tfrac{\omega^2}{c^2}\varepsilon)\phi_{\boldsymbol{k},\omega}(z) = -\frac{4\pi}{\varepsilon}\rho_{\boldsymbol{k},\omega}\delta(z), \tag{12}$$

$$(\partial_z^2 - k^2 + \tfrac{\omega^2}{c^2}\varepsilon)\boldsymbol{A}_{\boldsymbol{k},\omega}(z) = -\frac{4\pi}{c}\boldsymbol{j}_{\boldsymbol{k},\omega}\delta(z). \tag{13}$$

Solving Eqs.(12) and (13) for the z dependence gives

$$\phi_{\boldsymbol{k},\omega}(z) = \frac{2\pi\rho_{\boldsymbol{k},\omega}}{\varepsilon q(\omega)}e^{-q(\omega)|z|}, \quad \boldsymbol{A}_{\boldsymbol{k},\omega}(z) = \frac{2\pi\boldsymbol{j}_{\boldsymbol{k},\omega}}{cq(\omega)}e^{-q(\omega)|z|}, \tag{14}$$

with $q(\omega) = \sqrt{k^2 - \frac{\omega^2}{c^2}\varepsilon}$.

These relations must be combined with the current-field conductivity response relation

$$\boldsymbol{j}' = \sigma(\omega)\boldsymbol{E}. \tag{15}$$

Here the prime indicates induced current, whereas the quantities in Eq.(14) should be taken as sums of the external and induced contributions, $\rho = \rho' + \rho_{\rm ext}$, $\boldsymbol{j} = \boldsymbol{j}' + \boldsymbol{j}_{\rm ext}$. Writing $\boldsymbol{E} = -\nabla\phi - \frac{1}{c}\partial_t\boldsymbol{A}$ and using the continuity relations for the 2D currents and charges, $\rho_{k,\omega} = \frac{1}{\omega}\boldsymbol{k}\cdot\boldsymbol{j}_{k,\omega}$, we eliminate variables ρ and ϕ to obtain

$$\boldsymbol{j}'_{\boldsymbol{k},\omega} = i\omega\frac{2\pi\sigma(\omega)}{q(\omega)c^2}\left(\boldsymbol{j}_{\boldsymbol{k},\omega} - \frac{c^2}{\omega^2\varepsilon}\boldsymbol{k}\left(\boldsymbol{k}\cdot\boldsymbol{j}_{\boldsymbol{k},\omega}\right)\right), \tag{16}$$

with $\boldsymbol{j} = \boldsymbol{j}' + \boldsymbol{j}_{\rm ext}$. This relation can be put in the form of a 2×2 matrix response function, $\boldsymbol{j}'_{\boldsymbol{k},\omega} = M\left(\boldsymbol{j}'_{\boldsymbol{k},\omega} + \boldsymbol{j}^{\rm ext}_{\boldsymbol{k},\omega}\right)$. For longitudinal waves $\boldsymbol{j}_{\boldsymbol{k},\omega} \parallel \boldsymbol{k}$, $\boldsymbol{j}^{\rm ext}_{\boldsymbol{k},\omega} \parallel \boldsymbol{k}$ we obtain

$$\boldsymbol{j}_{\boldsymbol{k},\omega} = \frac{1}{1-M}\boldsymbol{j}^{\rm ext}_{\boldsymbol{k},\omega} = \frac{i\omega\varepsilon}{i\omega\varepsilon - 2\pi q(\omega)\sigma(\omega)}\boldsymbol{j}^{\rm ext}_{\boldsymbol{k},\omega}. \tag{17}$$

Dynamical compressibility can now be found by substituting in place of $\boldsymbol{j}^{\rm ext}_{\boldsymbol{k},\omega}$ the current induced by an external potential, $-i\sigma(\omega)\boldsymbol{k}\phi^{\rm ext}_{k,\omega}$. Relating the net current $\boldsymbol{j} = \boldsymbol{j}' + \boldsymbol{j}_{\rm ext}$ to the net charge as $\rho = \frac{1}{\omega}\boldsymbol{k}\cdot\boldsymbol{j}$ gives

$$\rho_{\omega,k} = \frac{k^2\sigma(\omega)\varepsilon}{i\omega\varepsilon - 2\pi q(\omega)\sigma(\omega)}\phi^{\rm ext}_{\omega,k}, \tag{18}$$

which is the result in Eq.(2) generalized to $\varepsilon \neq 1$. As a sanity check, at $\omega = 0$ we recover the standard result for an ideal conductor $\rho_k = -\frac{\varepsilon k}{2\pi}\phi_k$, where the minus sign describes perfect screening of an external potential by induced charges.

The result in Eq.(18) can be related to the $\varepsilon = 1$ result in Eq.(2) by absorbing ε into rescaled parameters,

$$c \to \tilde{c} = \frac{c}{\sqrt{\varepsilon}}, \quad \sigma_0 \to \tilde{\sigma}_0 = \frac{\sigma_0}{\varepsilon}, \tag{19}$$

upon which the dimensionless ratio $\alpha = 2\pi\sigma_0/c$ is reduced by a factor $\sqrt{\varepsilon}$. Accounting for this change, the results above can be applied directly, with the condition in Eq.(1) replaced by $\sigma_0 > \frac{\sqrt{\varepsilon}c}{2\pi}$, and so on. For a system of size $L = 20\,\mu$m, using the value $\varepsilon \approx 11$ (sapphire), the resonance frequency is $\omega_0 = \frac{\pi c}{\sqrt{\varepsilon}L} = 2\pi \times 2.26\,$THz. This value can be reduced by using proximal gates to screen the electron-electron interactions.

Lastly, we note that resonance sharpening, occurring when the collision rate γ exceeds resonance frequency, resembles motional narrowing in the hydrodynamic regime due to plasmon excitation being shared among many quickly relaxing degrees of freedom. This behavior can also be linked to the peculiar evolution of poles of the response function in the complex frequency plane. At small γ the poles represent the conventional collisionless plasmons. As γ grows, the poles move under the branch cuts, turning into tachyon modes with faster-than-c group velocity. Since the poles are positioned on the unphysical sheet of the complex frequency Riemann surface, they do not lead to propagating modes. However, they do influence the observable response through resonance sharpening and non-Lorentzian lineshapes. These features, along with a characteristic nonmonotonic dependence on experimental knobs, provide clear signatures of the tachyon regime.

We are grateful to I. V. Kukushkin and K. E. Nagaev for useful discussions.

[1] B. Wunsch, T. Stauber, F. Sols, F. Guinea, Dynamical polarization of graphene at finite doping. New J. Phys. **8**, 318 (2006).

[2] E. H. Hwang, S. Das Sarma, Dielectric function, screening, and plasmons in two-dimensional graphene. Phys. Rev. B **75**, 205418 (2007).

[3] M. Jablan, H. Buljan, M. Soljacic, Plasmonics in graphene at infrared frequencies. Phys. Rev. B **80**, 245435 (2009).

[4] F. H. L. Koppens, D. E. Chang, and F. J. Garcia de Abajo, Graphene Plasmonics: A Platform for Strong Light-Matter Interactions Nano Lett. **11** (8), 3370-3377 (2011).

[5] P. A. D. Goncalves and N. M. R. Peres, An Introduction to Graphene Plasmonics (Word Scientific, Singapore, 2016).

[6] D. N. Basov, M. M. Fogler, F. J. Garcia de Abajo, Polaritons in van der Waals materials, Science **354**, 195 (2016).

[7] J. Chen, M. Badioli, P. Alonso-Gonzalez, S. Thongrattanasiri, F. Huth, J. Osmond, M. Spasenovic, A. Centeno, A. Pesquera, P. Godignon, A. Zurutuza, N. Camara, F J. Garcia De Abajo, R. Hillenbrand, F. H. L. Koppens, Optical Nano-Imaging of Gate-Tunable Graphene Plasmons, Nature **487**, 77 (2012).

[8] Z. Fei, A. S. Rodin, G. O. Andreev, W. Bao, A. S. McLeod, M. Wagner, L. M. Zhang, Z. Zhao, M. Thiemens, G. Dominguez, M. M. Fogler, A. H. Castro Neto, C. N. Lau, F. Keilmann, D. N. Basov, Gate-Tuning of Graphene Plasmons Revealed by Infrared Nano-Imaging, Nature **487**, 82 (2012).

[9] G. F. Giuliani and G. Vignale, Quantum Theory of the Electron Liquid (Cambridge University Press, Cambridge, 2005).

[10] I. V. Kukushkin, J. H. Smet, S. A. Mikhailov, D. V. Kulakovskii, K. von Klitzing, and W. Wegscheider, Observation of Retardation Effects in the Spectrum of Two-Dimensional Plasmons, Phys. Rev. Lett. **90**, 156801 (2003).

[11] V. M. Muravev, P. A. Gusikhin, I. V. Andreev, and I. V. Kukushkin, Novel Relativistic Plasma Excitations in a Gated Two-Dimensional Electron System Phys. Rev. Lett. **114**, 106805 (2015).

[12] P. A. Gusikhin, V. M. Muravev, A. A. Zagitova, I. V. Kukushkin, Drastic Reduction of Plasmon Damping in Two-Dimensional Electron Disks, Phys. Rev. Lett. **121**, 176804 (2018).

[13] V. I. Falko and D. E. Khmelnitskii, What if the film conductivity is higher than the speed of light? Zh. Eksp. Teor. Fiz. **95**, 1988 (1989) [Sov. Phys. JETP **68**, 1150 (1989)].

[14] Resistance value in Eq.(1) can be estimated by combining the fine structure constant $\alpha = e^2/\hbar c \approx 1/137$ and the von Klitzing resistance quantum $h/e^2 = 25.8\,\mathrm{k}\Omega$. The quantity $2\pi/c$ then translates into resistance of $2\pi(e^2/\hbar c)(\hbar/e^2) \approx 188\,\Omega$ per square.

[15] V. A. Volkov, V. N. Pavlov, Radiative Plasmon Polaritons in Multilayer Structures with a Two-Dimensional Electron Gas, JETP Lett. **99**, 93-98 (2014).